DNA Nanotechnology | Hot Paper

DOI: 10.1002/ange.201410779

Antibody Activation using DNA-Based Logic Gates**

*Brian M. G. Janssen, Martijn van Rosmalen, Lotte van Beek, and Maarten Merkx**

Abstract: *Oligonucleotide-based molecular circuits offer the exciting possibility to introduce autonomous signal processing in biomedicine, synthetic biology, and molecular diagnostics. Here we introduce bivalent peptide–DNA conjugates as generic, noncovalent, and easily applicable molecular locks that allow the control of antibody activity using toehold-mediated strand displacement reactions. Employing yeast as a cellular model system, reversible control of antibody targeting is demonstrated with low nM concentrations of peptide–DNA locks and oligonucleotide displacer strands. Introduction of two different toehold strands on the peptide–DNA lock allowed signal integration of two different inputs, yielding logic OR- and AND-gates. The range of molecular inputs could be further extended to protein-based triggers by using protein-binding aptamers.*

Their synthetic accessibility and highly predictable binding properties make oligonucleotides (ODNs) ideal building blocks to construct molecular logical circuits.[1,2] The principle of toehold-mediated strand exchange[3,4] has proven particularly versatile, allowing the construction of robust circuits with a broad range of functionalities, including logic gates, signal amplification, signal thresholding, feedback control, and consensus gating.[5–10] Oligonucleotide-based circuits can also be integrated in biological systems, enabling the introduction of autonomous decision making in biomedicine, synthetic biology, and molecular diagnostics.[11–14] However, such applications are still limited by a lack of generic approaches to interface ODN circuits with protein activity.[15,16] So far, most examples to control protein activity using ODN-based circuits are based on the streptavidin–biotin interaction[17,18] or use a limited number of protein-binding aptamers.[19–23] Here we introduce a generic and easily applicable approach to use the output of DNA/RNA-based logic operations to control the activity of antibodies.

Antibody-based molecular recognition plays a dominant role in the life sciences ranging from applications in diagnostics and molecular imaging to antibody-based therapy and targeted drug delivery. To increase the specificity of antibody-based molecular recognition, new strategies are required to make antibody activity controllable by the presence of other biomarkers such as microRNAs, enzyme activity, and cell surface receptors.[24,25] In an impressive display of molecular engineering the group of Church used DNA origami to construct a locked DNA barrel (NanoRobot) to shield specific antibodies. Binding of platelet-derived growth factor and several receptor-based biomarkers to aptamer-based locks on the NanoRobot, resulted in the opening of the DNA box, allowing the antibodies to bind to cell surface receptors.[21] Our group recently reported a generic and noncovalent strategy to block antibody targeting by making use of bivalent peptide–DNA conjugates. These self-assembling bivalent ligands can effectively bridge the two antigen binding sites present in monoclonal antibodies, which allowed control of antibody-based targeting in a protease-reversible manner.[24] We realized that the use of dsDNA as a linker in bivalent peptide ligands provides an excellent opportunity to use the output of DNA-based logic operations to control the activity of antibodies (Scheme 1).

To explore the design principles for DNA-based control of antibody activation, we used an IgG_1-type monoclonal antibody against the hemagglutinin (HA) epitope YPYDVPDY. This peptide epitope is derived from the influenza virus and binds to an anti-HA antibody with a monovalent affinity of 5 nM.[26] Bivalent peptide–dsDNA conjugates were synthesized with DNA linkers consisting of 20 or 35 bp, with one of the strands containing an additional 8 base toehold sequence to facilitate strand displacement (Figures S1–S3). Bi- or monovalent peptide–dsDNA ligands were obtained by hybridization of complementary (peptide-functionalized) ODN strands (Figure 1a). Analysis using size exclusion chromatography showed that addition of one equivalent of

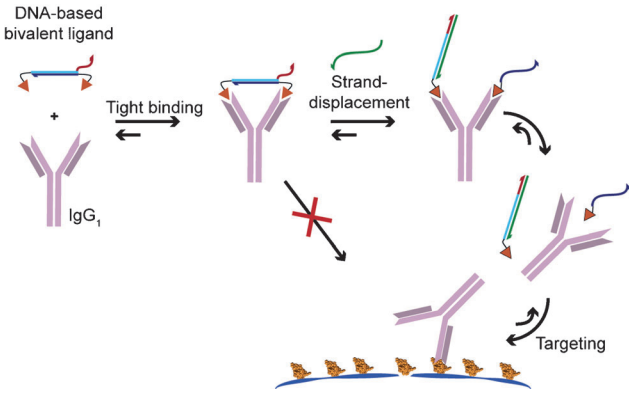

Scheme 1. Blocking antibodies using bivalent peptide–dsDNA conjugates allows reversible control of antibody targeting using toehold-mediated strand displacement. Disruption of the dsDNA linker generates more weakly binding monovalent peptide ligands, which dissociate to allow target binding.

[*] B. M. G. Janssen, M. van Rosmalen, L. van Beek, Dr. M. Merkx
Laboratory of Chemical Biology and Institute for Complex Molecular Systems, Eindhoven University of Technology
De Rondom 70, 5612 AP Eindhoven (The Netherlands)
E-mail: m.merkx@tue.nl

[**] We thank Dr. Tom de Greef for stimulating discussions. This work was supported by NanoNextNL, a micro- and nanotechnology consortium of the Government of the Netherlands and 130 partners, and by an ERC starting grant (ERC-2011-StG 280255).

Supporting information for this article is available on the WWW under http://dx.doi.org/10.1002/anie.201410779.

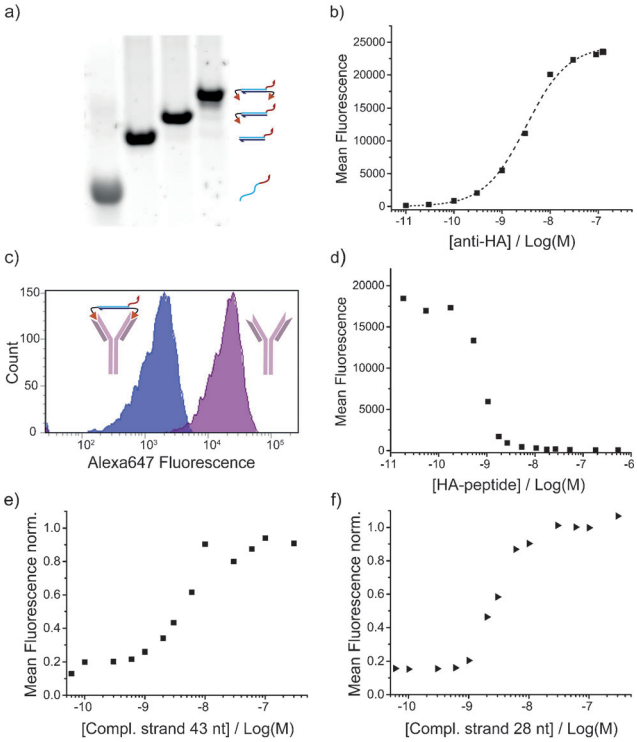

Figure 1. Antibody activation by toehold-mediated DNA strand displacement. a) Native 15% polyacrylamide gel showing formation of non-, mono- and bivalent peptide–DNA ligands (35DS0x, 35DS1x, and 35SMD2x) consisting of a 35 bp dsDNA and an 8 base toehold. b) Titration experiment monitoring the binding of Alexa647-labeled anti-HA antibody to yeast cells displaying the HA-epitope. c) Histogram showing Alexa647 fluorescence for yeast cells incubated with 1 nM Alexa647-labeled anti-HA antibody in the presence or absence of 1 nM 35SMD2x. d) Titration experiment showing binding of anti-HA antibody (1 nM) as a function of the concentration of the bivalent peptide–DNA ligand 35SMD2x. e,f) Titration experiments showing restoration of antibody binding as a function of displacer strand concentration. Different concentrations of displacer strands (43 or 28 nucleotides, resp. ODN-11 or -12) were added to 1 nM anti-HA antibody and 1.1 nM bivalent ligand [35SMD2x (e) or 20SMD2x (f)] and incubated for 2 h prior to FACS analysis. The mean fluorescence was normalized by dividing it by the mean fluorescence observed in the presence of 1.1 nM of the corresponding monovalent ligand (35DS1x or 20DS1x).

bivalent peptide–dsDNA ligand to the antibody resulted in the formation of a cyclic 1:1 complex, as expected for strong bivalent binding (Figure S4).

To verify efficient blocking of antibody targeting by the bivalent peptide–DNA locks, yeast cells were used that display the HA epitope fused to the yellow fluorescent protein Citrine (Figure S5). This system allows quantitative monitoring of cell-surface antibody binding by flow-cytometric analysis of the amount of fluorescently labeled antibody binding to Citrine-positive (and thus HA-displaying) yeast cells. Monitoring the amount of cell-bound Alexa647-labeled anti-HA antibody as a function of antibody concentration yielded a K_d of 6.3 ± 0.3 nM (Figure 1b), which is in good agreement with titration experiments using fluorescently labeled peptide.[26] Next, the concentration of anti-HA antibody was kept at 1 nM, while changing the amount of bivalent peptide–dsDNA lock. Only a slight excess of the bivalent peptide–DNA lock already completely blocked the binding of fluorescence-labeled antibody to HA-tag-displaying yeast cells, showing that the interaction between the bivalent peptide–dsDNA ligand and the antibody is very strong (Figure 1c,d). To test whether the bivalent interaction can be disrupted by toehold-mediated strand displacement, a fully complementary oligonucleotide strand was titrated to the blocked antibody (1 nM antibody and 1.1 nM bivalent-peptide–dsDNA) and the reactivation of antibody targeting was monitored using fluorescence-activated cell sorting (FACS). To ensure complete thermodynamic equilibration, the displacement reaction was incubated for 2 h prior to FACS analysis. Figure 1e and 1f show that antibody binding can be completely restored by addition of low nM concentrations of the displacer strand. The final binding level is comparable to that obtained using the same concentrations of antibody and monovalent peptide–dsDNA. Similar results were obtained for locks containing 20 bp and 35 bp dsDNA linkers, which shows that the flexibility in the hinge region allows the antibody to accommodate different lengths of dsDNA linker (7 and 12 nm, respectively), as previously observed for an anti-HIV1-p17 antibody.[24] This flexibility is important, because it allows more design freedom when targeting different oligonucleotide inputs or more complicated logic gates. In subsequent experiments we continued with the 20 bp dsDNA linker.

The experiments above show that an eight nucleotide toehold provides sufficient thermodynamic driving force to overcome the favorable bivalent interaction between the antibody and the bivalent peptide–dsDNA lock. To assess whether the kinetics of the strand displacement reaction are affected by binding to the antibody, a fluorophore-quencher pair was introduced in the bivalent-dsDNA lock (20FQ2x) to allow direct monitoring of strand displacement using fluorescence (Figures 2 and S9). The pseudo first order rate constant of the displacement reaction was measured as a function of toehold length and displacer strand concentration. Surprisingly, very similar reaction rates were observed in the absence and presence of antibody (Figure 2). When using short toehold lengths and/or low concentrations of the displacer strand, the rate is determined by formation of the toehold complex, whereas the DNA-displacement reaction itself becomes rate-limiting at a toehold size of >8 nt and/or high concentrations of the input strand.[6,27] The similar kinetics thus suggest that invasion of the displacer strand is not hampered by binding of the peptide–DNA lock to the antibody and can freely rotate around the dsDNA linker during the strand displacement reaction.

Having established the principle of antibody activation using a single input strand, we next rendered antibody activation conditional on the presence of two oligonucleotides. To this end we constructed DNA-based bivalent ligands containing a 10 nucleotides single strand toehold at each side of a 20 bp dsDNA linker (Figure 3a). Depending on the length of the overlapping sequences, this architecture could act as either an AND- or an OR-gate. As expected, addition of one of the fully complementary 30 bp input strands was sufficient to fully restore antibody targeting, representing an

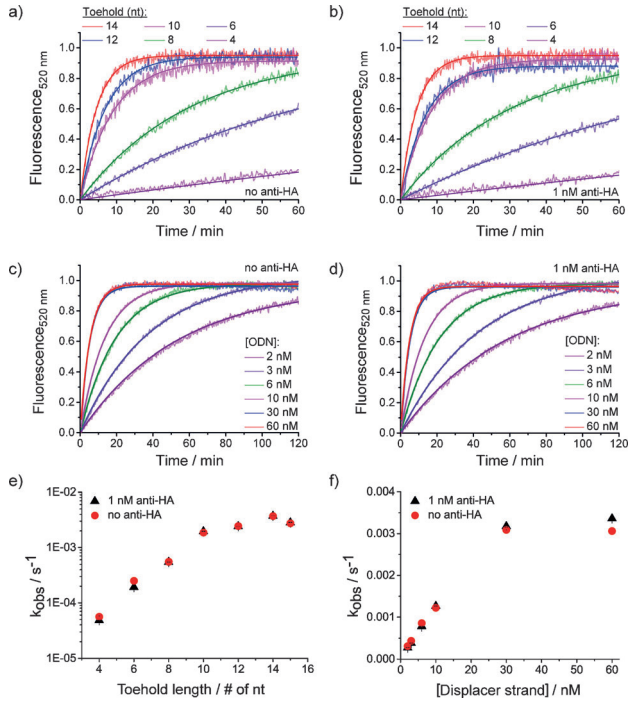

Figure 2. Kinetics of the toehold-mediated strand displacement reaction in the absence (a and c) and presence of 1 nM anti-HA antibody (b and d) as a function of toehold length (a and b) and displacement strand concentration (c and d). All displacement reactions were performed in standard TE-buffer (pH 8.0) including 12.5 mM $MgCl_2$ using 1 nM 20FQ2x by monitoring the increase of fluorescence in time. The effect of toehold length was studied using 4 nM of the displacer strand. The effect of displacer strand concentration was studied using a constant toehold length of eight nucleotides (ODN-34). Pseudo first order reaction rates derived from these experiments were plotted as function of toehold length (e) or as function of displacer strand concentration (f).

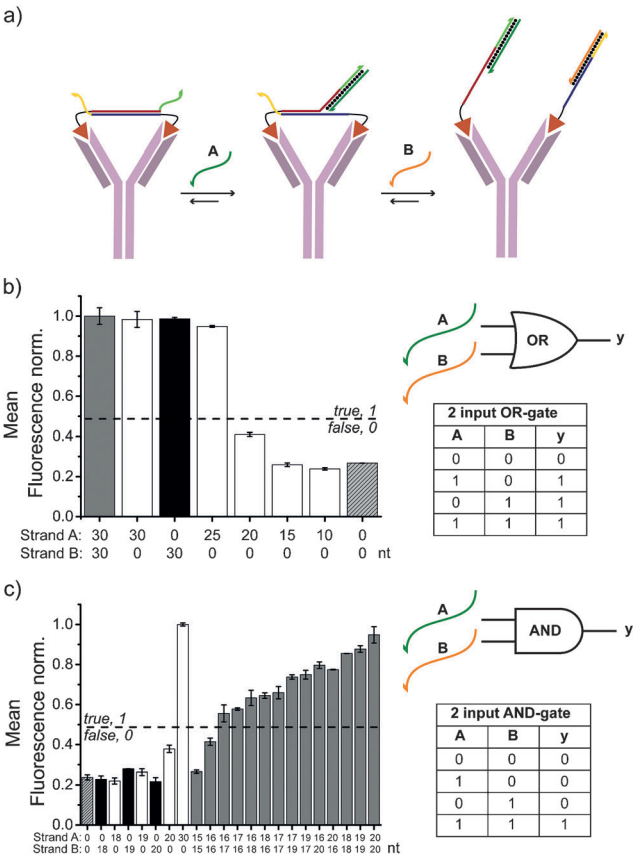

Figure 3. a) Control of antibody activity using two inputs yielding logic OR- or AND-gates. 1 nM anti-HA antibody was blocked by addition of 1.1 nM of a bivalent ligand consisting of a 20 bp linker (20LG2x), flanked by two 10 nt single-strand overhangs. Following incubation with 24 nM input strand(s) for 2 h, yeast cells were added and antibody binding was monitored by measuring the mean cellular Alexa647 fluorescence. b) OR-gate behavior is observed for input strands with more than 20 nucleotides. c) AND-gate behavior for combinations of two input strands depends on the length of the strands. All experiments were performed in duplo. A strand length of 0 nt means that no displacer strand was added. The true/false threshold was defined by taking the square root of the product of the maximum and the minimum outputs.[28]

OR-gate (Figure 3b). OR-gate behavior was also observed for 25 nucleotides input strands, but only a small amount of activation was observed using a single 20 nucleotides strand (complementary to the 10 nucleotides toehold and 10 bp in the linker) even in the presence of a 20-fold excess of the input strand (Figure 3b). The background of 0.2 fluorescence units that was observed even in the absence of displacer strands is a consequence of the small excess of bivalent peptide–DNA lock that was used (1.1 nM versus 1 nM antibody), which results in a small amount of non-blocked antibody (see also Figure 1d). To identify the regime in which the system shows AND-gate behavior, we systematically varied the lengths of the two input strands between 15 and 20 nucleotides in steps of 1 nt. Figure 3c shows that addition of two 15 nucleotide strands is not sufficient to disrupt antibody blockage. In this case, strand invasion probably occurs, but the 10 bp that remain between the two linker strands are sufficient to preserve the bivalent ligand. However, increasing the number of nucleotides further rapidly increases the amount of antibody activation, showing partial antibody activation by two 16 nucleotide strands and nearly complete activation using two 17 nucleotide strands. The sharp transition between inhibition and activation is attractive because it allows the design of AND-gates with minimal leakage. It also provides maximal flexibility with respect to the length and sequence of the two input strands, allowing the integration of the outputs from two different DNA-logic circuits or two different miRNA sequences as triggers in AND- or OR-gate designs.

To further expand the type of molecular triggers, we also explored the possibility to control antibody activity using protein-binding aptamers.[29–31] A previously reported high-affinity thrombin aptamer was extended at its 5′-end with six nucleotides (A) such that it could partially hybridize with the displacer strand (D), and thus prevent D from binding to the toehold in the bivalent peptide–DNA lock (20Apt2x). Binding of thrombin to the aptamer sequence should result in release of the displacer strand, allowing the displacer strand to bind to the toehold on the peptide–DNA lock, resulting in strand displacement and antibody activation. Monitoring the amount of antibody activation as a function of thrombin concentration showed a 2-fold increase in antibody targeting

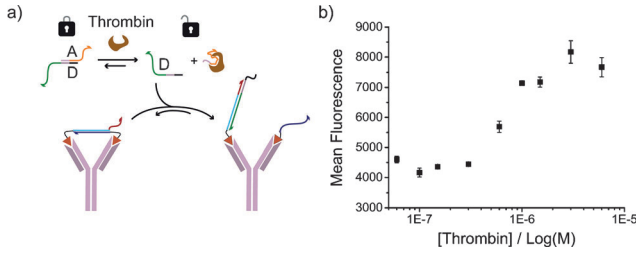

Figure 4. a) Principle of aptamer-mediated control of antibody reactivation. b) Titration experiment showing reactivation of antibody binding as a function of thrombin concentration. 1 nM of Alexa647-labeled anti-HA antibody and 1.1 nM 20Apt2x were incubated prior to the addition of the A:D complex (300 nM A and 100 nM D) and different concentrations of thrombin. All experiments were performed in duplo.

between 300 nM and 1 μM (Figure 4), whereas no activation was observed in control reactions with thrombin that lacked the aptamer–displacer complex or when the aptamer–displacer was made so stable that thrombin binding could not release the displacer strand (Figures S7 and S8). Addition of the aptamer–displacer complex in the absence of thrombin also resulted in a small increase in antibody activation, which could be partially repressed by using a three-fold excess of aptamer over displacer strand (300 nM A and 100 nM D, Figure S8). The modularity of the approach used here should allow the same locked antibody to be activated by different aptamers. For future applications the aptamer could also be directly included in the dsDNA linker, although this may require extensive reengineering of the peptide–DNA lock for each new aptamer.

In conclusion, bivalent peptide–dsDNA conjugates provide effective noncovalent molecular locks that allow control of antibody activity using toehold-mediated strand displacement reactions. This new approach takes advantage of the large difference in affinity between a bivalent peptide–DNA ligand and the monovalent peptide–DNA ligand that forms as a result of a strand displacement reaction. The most important design constraint is that the monovalent affinity of the antibody–epitope interaction should be significantly lower than the effective concentration provided by the dsDNA linker, which has been estimated to be approximately 10 μM,[24] but not so low as to block antibody binding to a cell surface receptor as a monovalent ligand. Our design compares favorably with strategies based on 3D DNA origami[21,32] in its ease of construction and the possibility to use hydrolytically stable ODN analogues such as phosphorothioate oligonucleotides[33] or peptide nucleic acids.[34] Because it is based on the characteristic Y-shaped molecular architecture shared by all antibodies, our approach provides a generic strategy to introduce autonomous signal processing in antibody-based targeting and exploit the molecular recognition properties of antibodies in the field of DNA-based computing.

Received: November 5, 2014
Published online: January 8, 2015

Keywords: antibodies · aptamers · DNA nanotechnology · molecular computing · peptide–oligonucleotide conjugates

[1] D. Han, H. Kang, T. Zhang, C. Wu, C. Zhou, M. You, Z. Chen, X. Zhang, W. Tan, *Chem. Eur. J.* **2014**, *20*, 5866 – 5873.
[2] M. N. Stojanovic, D. Stefanovic, S. Rudchenko, *Acc. Chem. Res.* **2014**, *47*, 1845 – 1852.
[3] B. Yurke, A. J. Turberfield, A. P. Mills, F. C. Simmel, J. L. Neumann, *Nature* **2000**, *406*, 605 – 608.
[4] A. J. Turberfield, J. C. Mitchell, B. Yurke, A. P. Mills, M. I. Blakey, F. C. Simmel, *Phys. Rev. Lett.* **2003**, *90*, 118102.
[5] D. Y. Zhang, A. J. Turberfield, B. Yurke, E. Winfree, *Science* **2007**, *318*, 1121 – 1125.
[6] D. Y. Zhang, E. Winfree, *J. Am. Chem. Soc.* **2009**, *131*, 17303 – 17314.
[7] L. Qian, E. Winfree, J. Bruck, *Nature* **2011**, *475*, 368 – 372.
[8] L. Qian, E. Winfree, *Science* **2011**, *332*, 1196 – 1201.
[9] Y.-J. Chen, N. Dalchau, N. Srinivas, A. Phillips, L. Cardelli, D. Soloveichik, G. Seelig, *Nat. Nanotechnol.* **2013**, *8*, 755 – 762.
[10] X. Ran, F. Pu, J. Ren, X. Qu, *Small* **2014**, *10*, 1500 – 1503.
[11] J. Hemphill, A. Deiters, *J. Am. Chem. Soc.* **2013**, *135*, 10512 – 10518.
[12] M. Rudchenko, S. Taylor, P. Pallavi, A. Dechkovskaia, S. Khan, V. P. Butler, Jr., S. Rudchenko, M. N. Stojanovic, *Nat. Nanotechnol.* **2013**, *8*, 580 – 586.
[13] F. Wang, C.-H. Lu, I. Willner, *Chem. Rev.* **2014**, *114*, 2881 – 2941.
[14] C. Jung, A. D. Ellington, *Acc. Chem. Res.* **2014**, *47*, 1825 – 1835.
[15] A. Prokup, A. Deiters, *Angew. Chem. Int. Ed.* **2014**, *53*, 13192 – 13195; *Angew. Chem.* **2014**, *126*, 13408 – 13411.
[16] B. M. G. Janssen, W. Engelen, M. Merkx, *ACS Synth. Biol.* **2014**, DOI: 10.1021/sb500278z.
[17] F. Li, H. Zhang, Z. Wang, X. Li, X.-F. Li, X. C. Le, *J. Am. Chem. Soc.* **2013**, *135*, 2443 – 2446.
[18] Z. Zhang, C. Hejesen, M. B. Kjelstrup, V. Birkedal, K. V. Gothelf, *J. Am. Chem. Soc.* **2014**, *136*, 11115 – 11120.
[19] P. S. Lau, B. K. Coombes, Y. Li, *Angew. Chem. Int. Ed.* **2010**, *49*, 7938 – 7942; *Angew. Chem.* **2010**, *122*, 8110 – 8114.
[20] J. Elbaz, O. Lioubashevski, F. Wang, F. Remacle, R. D. Levine, I. Willner, *Nat. Nanotechnol.* **2010**, *5*, 417 – 422.
[21] S. M. Douglas, I. Bachelet, G. M. Church, *Science* **2012**, *335*, 831 – 834.
[22] D. Han, Z. Zhu, C. Wu, L. Peng, L. Zhou, B. Gulbakan, G. Zhu, K. R. Williams, W. Tan, *J. Am. Chem. Soc.* **2012**, *134*, 20797 – 20804.
[23] M. You, L. Peng, N. Shao, L. Zhang, L. Qiu, C. Cui, W. Tan, *J. Am. Chem. Soc.* **2014**, *136*, 1256 – 1259.
[24] B. M. G. Janssen, E. H. M. Lempens, L. L. C. Olijve, I. K. Voets, J. L. J. van Dongen, T. F. A. de Greef, M. Merkx, *Chem. Sci.* **2013**, *4*, 1442 – 1450.
[25] L. R. Desnoyers, O. Vasiljeva, J. H. Richardson, A. Yang, E. E. M. Menendez, T. W. Liang, C. Wong, P. H. Bessette, K. Kamath, S. J. Moore, et al., *Sci. Transl. Med.* **2013**, *5*(207), 1 – 10.
[26] S. Banala, S. J. A. Aper, W. Schalk, M. Merkx, *ACS Chem. Biol.* **2013**, *8*, 2127 – 2132.
[27] N. Srinivas, T. E. Ouldridge, P. Šulc, J. M. Schaeffer, B. Yurke, A. A. Louis, J. P. K. Doye, E. Winfree, *Nucleic Acids Res.* **2013**, *41*, 10641 – 10658.
[28] M. P. Nikitin, V. O. Shipunova, S. M. Deyev, P. I. Nikitin, *Nat. Nanotechnol.* **2014**, *9*, 716 – 722.
[29] L. C. Bock, L. C. Griffin, J. A. Latham, E. H. Vermaas, J. J. Toole, *Nature* **1992**, *355*, 564 – 566.
[30] R. Nutiu, Y. Li, *J. Am. Chem. Soc.* **2003**, *125*, 4771 – 4778.
[31] N. Li, C.-M. Ho, *J. Am. Chem. Soc.* **2008**, *130*, 2380 – 2381.
[32] J. Hahn, S. F. J. Wickham, W. M. Shih, S. D. Perrault, *ACS Nano* **2014**, *8*, 8765 – 8775.
[33] F. Abendroth, O. Seitz, *Angew. Chem. Int. Ed.* **2014**, *53*, 10504 – 10509; *Angew. Chem.* **2014**, *126*, 10672 – 10677.
[34] U. Koppelhus, P. E. Nielsen, *Adv. Drug Delivery Rev.* **2003**, *55*, 267 – 280.

